Original Article

Islet Inflammation and Fibrosis in a Spontaneous Model of Type 2 Diabetes, the GK Rat

Françoise Homo-Delarche,[1] Sophie Calderari,[1] Jean-Claude Irminger,[2] Marie-Noëlle Gangnerau,[1] Josiane Coulaud,[1] Katharina Rickenbach,[2] Manuel Dolz,[1] Philippe Halban,[2] Bernard Portha,[1] and Patricia Serradas[1]

The molecular pathways leading to islet fibrosis in diabetes are unknown. Therefore, we studied gene expression in islets of 4-month-old Goto-Kakizaki (GK) and Wistar control rats. Of 71 genes found to be overexpressed in GK islets, 24% belong to extracellular matrix (ECM)/cell adhesion and 34% to inflammatory/immune response families. Based on gene data, we selected several antibodies to study fibrosis development during progression of hyperglycemia by immunohistochemistry. One-month-old GK and Wistar islets appeared to be similar. Two-month-old GK islets were strongly heterogenous in terms of ECM accumulation compared with Wistar islets. GK islet vascularization, labeled by von Willebrand factor, was altered after 1 month of mild hyperglycemia. Numerous macrophages (major histocompatibility complex class II$^+$ and CD68$^+$) and granulocytes were found in/around GK islets. These data demonstrate that marked inflammatory reaction accompanies GK islet fibrosis and suggest that islet alterations in this nonobese model of type 2 diabetes develop in a way reminiscent of microangiopathy. *Diabetes* 55:1625–1633, 2006

Islet fibrosis has been observed in humans and also in various spontaneous rodent models of type 2 diabetes, with or without obesity. In 4-month-old diabetic nonobese Goto-Kakizaki (GK) rats, Kakizaki et al. (1) first described the presence of large islets where endocrine cells were disrupted by fibrotic tissue ("starfish-like islets"), which later was confirmed by other groups (2,3). In nondiabetic Zucker fatty rats, occasional fibrotic and irregular islets are seen by 12 weeks of age (4), while these fibrotic islets are more frequent in younger (5- to 7-week-old) Zucker diabetic fatty (ZDF) rats. By 12 weeks of age, many ZDF rat islets are markedly abnormal with fibrosis and irregular projections in the exocrine tissue (4). The Otsuka Long-Evans Tokushima fatty (OLETF) rats also show disorganized fibrotic islets with vessel anomalies (5). A more recently established inbred strain, the spontaneously diabetic Torii (SDT) rat, develops hyperglycemia without obesity after 20 weeks of age (6). The primary changes of SDT islets consist of microvascular events at 8–10 weeks. At that time, SDT rats have lower plasma insulin and lower β-cell mass. These vascular alterations are followed by inflammation and progressive fibrosis and eventually islet atrophy. Islet architectural changes are also observed in type 2 diabetic mice, in association with presence of inflammatory cells and some extracellular matrix (ECM) deposition (7).

In humans, amyloid deposition leads to morphological islet alterations close to those observed in spontaneous rat type 2 diabetic models (8). Amyloid can be observed as perivascular deposits adjacent to capillaries surrounding the islet and also adjacent to capillaries penetrating the islet core. The most extensive islet amyloid deposits are associated with decreased β-cell mass (8).

Fibrosis is usually a consequence of an inflammatory reaction. Taking into account the increasing role of inflammation in type 2 diabetes pathogenesis (9,10), we investigated in greater depth islet alterations occurring in GK rats, a type 2 diabetes model that we have previously and extensively studied from fetal life onwards (2,11,12). Before birth, GK rats present decreased β-cell mass and low plasma insulin as compared with Wistar control rats. Then, they develop mild hyperglycemia and insulin resistance around weaning (3–4 weeks of age). Here, using a complementary approach that associated gene expression analysis (Affymetrix microarrays), quantitative RT-PCR, and immunohistochemical studies of pancreata as a function of hyperglycemia duration, we demonstrate that an inflammatory reaction is associated with islet fibrosis in 4-month-old diabetic GK rats according to a process reminiscent of microangiopathy. These alterations worsened with hyperglycemia duration and might contribute to enhanced GK β-cell impairment.

RESEARCH DESIGN AND METHODS

For gene analysis and immunohistochemistry, experimentation was conducted on fed 15- to 16-week-old and 4-, 8-, and 16-week-old male GK rats and age- and sex-matched nondiabetic Wistar rats from our local colonies, respectively. The characteristics of the nonobese GK rat model of type 2 diabetes maintained in our colony at University Paris 7 have been described previously (12). Glycemia was determined with a glucose analyzer (Beckman). At 1 (unweaned animals), 2, and 4 months of age, basal morning blood glucose levels were: 6.6 ± 0.2 and 10.8 ± 0.5 mmol/l (n = 5–8, $P < 0.001$), 7.3 ± 0.3 and 10.7 ± 0.8 mmol/l (n = 6–7, $P < 0.01$), and 6.5 ± 0.3 and 11.9 ± 0.8 mmol/l (n = 5–7, $P < 0.002$), for Wistar and GK rats, respectively (unpaired Student's t test). Animal experimentation was performed in accordance with accepted

From the [1]Unité Mixte de Recherche 7059, National Center for Scientific Research, Diderot University, Paris, France; and the [2]Department of Genetic Medecine and Development, University Medical Center, Geneva, Switzerland.

Address correspondence and reprint requests to Francoise Homo-Delarche, CNRS UMR 7059, Université Paris 7/D. Diderot, 2, place Jussieu, 75005 Paris, France. E-mail: francoise.homo-delarche@paris7.jussieu.fr.

Received for publication 23 November 2005 and accepted in revised form 27 February 2006.

F.H.-D., S.C., and J.-C.I. contributed equally to this work.

ECM, extracellular matrix; MHC, major histocompatibility complex; vWF, von Willebrand factor.

DOI: 10.2337/db05-1526

TABLE 1
Primer oligonucleotide sequences

	Sequences
Annexin 1/lipocortin 1	Forward: 5′ CCT GGA GGA GGT TGT TTT GG 3′
Annexin 1	Reverse: 5′ CAG CAC GGA GTT CAT CTG CAT 3′
CD53	Forward: 5′ GCG TGG TTT CAC TCC AAT TTC 3′
CD53	Reverse: 5′ GGA CAT CCC CAG CAC CTG TA 3′
CD74	Forward: 5′ CCA GGA CCA CGT GAT GCA 3′
CD74	Reverse: 5′ CCC CTT CAG CTG TGG GTA GTT 3′
Collagen type I	Forward: 5′ CCC AAC CCC CAA AAA CG 3′
Collagen type I	Reverse: 5′ CTG CGT CTG GTG ATA CAT ATT CTT CT 3′
Collagen type III	Forward: 5′ AGC TGG CCT TCC TCA GAC TTC 3′
Collagen type III	Reverse: 5′ GCT GTT TTT GCA GTG GTA TGT AAT G 3′
Decorin	Forward: 5′ GCG GCA ACC CAC TGA AAA 3′
Decorin	Reverse: 5′ TGT ATC CGA GAC CCT TCA TTC C 3′
Fibronectin	Forward: 5′ CCT ACG GAT GAC TCA TGC TTT G 3′
Fibronectin	Reverse: 5′ CAG ATA ACC GCT CCC ATT CC 3′
Glutathione peroxidase	Forward: 5′ TGC TCA TTG AGA ATG TCG CG 3′
Glutathione peroxidase	Reverse: 5′ TGT AGT CCC GGG TCG TGG T 3′
Lipocaline 2	Forward: 5′ TCC GAT GAA CTG AAG GAG CG 3′
Lipocaline 2	Reverse: 5′ GAG GCC CAG AGA CTT GGC A 3′
Lipopolysaccharide-induced tumor necrosis factor α	Forward: 5′ TGG CTC TCC TGT GGC AGT CT 3′
Lipopolysaccharide-induced tumor necrosis factor α	Reverse: 5′ CGC AAA ACG GAA TGA AGC A 3′
MHC class II	Forward: 5′ CCC TCC AGC GGT CAA TGT 3′
MHC class II	Reverse: 5′ TGA CAC GCC TTT GGT GAC A 3′
Membrane type 1-matrix metalloproteinase	Forward: 5′ GCC ATC ATG GCT CCC TTT TA 3′
Membrane type 1-matrix metalloproteinase	Reverse: 5′ GCG GCG ATC GTC ATC AG 3′
Osteopontin	Forward: 5′ CCT TCA CTG CCA GCA CAC AA 3′
Osteopontin	Reverse: 5′ CCG TCA GGG ACA TCG ACT GT 3′
Tissue inhibitor of metalloproteinase-1	Forward: 5′ CCG CAG CGA GGA GTT TCT C 3′
Tissue inhibitor of metalloproteinase-1	Reverse: 5′ GGC AGT GAT GTG CAA ATT TCC 3′
Vdup1 (or thioredoxin-interacting protein)	Forward: 5′ GCA AGA GTC TCC GAG TGC AGA 3′
Vdup1	Reverse: 5′ TGT TGC AGC CCA GAA TGG A 3′

standards of animal care as established in the French National Center for Scientific Research guidelines.

Islet isolation. Rats were injected intraperitoneally with pentobarbital sodium (1 ml/kg body wt; Ceva Santé Animale, Libourne, France). For glycemia determination, blood samples were collected after decapitation and immediately centrifuged at 4°C. Pancreata were digested with collagenase according to standard procedures. Subsequently, islets were purified using a continuous Histopaque (Sigma, St. Louis, MO) gradient. Purified islet fractions were collected, and all islets (i.e., islets with normal architecture and islets more or less affected by fibrosis) were hand picked up under a stereomicroscope and lysate. The homogenized lysate was conserved at −80°C until RNA extraction. Six to 16 different islet isolation were done for Wistar and GK rats ($n = 20$ Wistar and $n = 50$ GK) with islet recovery per rat of 307 ± 32 and 72 ± 14, respectively.

RNA preparation and differential gene expression by cDNA analysis. RNA was extracted from Wistar and GK islets using the RNeasy total RNA Isolation Kit (Qiagen, Hilder, Germany). Using the Superscript Choice System (Invitrogen, Groningen, Netherlands), 7 μg RNA was used to synthesize double-stranded cDNA. In vitro transcription was carried out on 6 μl cDNA using Bioarray High Yield RNA transcript-labeling reagents (Enzo Diagnostics, New York, NY). Reactions yielded 50–70 μg biotin-labeled cRNA, which was purified on RNeasy affinity columns (Qiagen) and fragmented at 94°C for 35 min in fragmentation buffer as previously described (13). Then, 15–20 μg fragmented cRNA was hybridized to the Affymetrix RG-U34A oligonucleotide microarrays representative of 8,799 rat genes. Arrays were scanned, and the data obtained were analyzed using Microarray suite 5.0, Affymetrix Data Mining tool 2.0, and Genespring 6 (Agilent Technologies, Palo Alto, CA). The microarray experiments were performed in collaboration with the Genomics Platform of the NCCR Frontiers, Geneva. Gene expression was determined relative to the housekeeping genes glyceraldehyde-3-phosphate dehydrogenase and the ribosomal gene L3. Genes were considered up- or downregulated if the averaged fold change was at least two in duplicate experiments. Genes were assigned to functional groups by database searches on PubMed and Affymetrix websites.

Quantitative RT-PCR. RNA was isolated using RNeasy Mini kit (Qiagen). cDNA was synthesized with Superscript II (Invitrogen, Basel, Switzerland), using 1 μg of total RNA in a 20-μl reaction volume. The dsDNA-specific dye SYBR Green I (Eurogentech, Bruxels, Belgium) and fluorescein (Biorad, Hercules, CA) were incorporated into the PCR buffer (qPCR core kit, Eurogentech) to allow for quantitative detection of the PCR product (for primers see Table 1). The results were analyzed using the iCycler iQ System (Biorad). The housekeeping genes glyceraldehyde-3-phosphate dehydrogenase and ribosomal protein (L3) were used as internal controls.

Immunohistochemistry. For insulin labeling, pancreata from Wistar and GK rats were excised, fixed in aqueous Bouin's solution, and embedded in paraplast, according to standard procedures. Histological sections of pancreas (7-μm thick) were prepared and mounted on glass microscope slides (Superfrost Plus, Kindler O, Freiburg, Germany). Slides were incubated overnight at 4°C in a humidified chamber with guinea pig anti-porcine insulin. For insulin detection, a peroxidase-conjugated rabbit anti–guinea pig IgG was used (for antibodies see Table 2). After washing, peptide immunoreactivity was localized with 3,3′-diaminobenzidine-tetra-hydrochloride using a peroxidase substrate kit (DAB; Vector Laboratories, Burlingame, CA). Tissue sections were counterstained with hematoxylin and mounted under glass coverslips.

For ECM protein and immune cell labeling, pancreata were removed, embedded in optimal cutting temperature (Tissue-Tek, Miles, Elkart, IN), and frozen in n-hexane on dry ice–chilled alcohol. Tissues were stored at −80°C until immunohistochemistry was performed. For 10 min, 6-μm thick cryostat sections were fixed in acetone. After washing with PBS containing 0.05% Tween-20 (Merck, Paris, France) (PBS/Tween), slides were incubated with primary antibodies for 30 min at room temperature in a moist chamber. Subsequently, slides were washed twice with PBS/Tween and incubated with appropriate peroxidase-coupled secondary antibodies in the absence or presence of 1% normal rat serum for 30 min at room temperature (for antibodies see Table 2). Following further PBS/Tween washing, slides were incubated with 3-amino-9-ethylcarbazole (Sigma, Saint-Quentin-Fallavier, France) as the substrate in 50 mmol/l sodium acetate and 0.02% H_2O_2 and washed in water after 3 min. Finally, slides were counterstained for 3 min in Harri's hematoxylin (Merck), dehydrated in serially graded ethanol baths, and mounted. For each series of pancreas sections, one slide was stained only with the second antibody as a control for endogenous peroxidase activity and nonspecific antibody binding.

TABLE 2
List of antibodies

Antibodies	Specificity	Supplier	Dilution
Primary antibodies			
Collagen I	Rabbit anti-rat	Novotec	1:40
Collagen IIII	Rabbit anti-rat	Novotec	1:50
Fibronectin	Rabbit anti-rat	Novotec	1:40
Insulin	Guinea pig anti-porcine	ICN Pharmaceuticals	1:1000
vWF	Rabbit anti-human	DakoCytomation	1:100
MHC class II	Mouse anti-mouse/rat I-A	Serotec	1:300
ED1	Mouse anti-rat CD68	Serotec	1:100
ED2	Mouse anti-rat CD153	BMA Biomedicals	1:500
ED3	Mouse anti-rat CD169	BMA Biomedicals	1:500
CD53	Mouse anti-rat	Serotec	1:30
Granulocytes	Mouse anti-rat	Serotec	1:30
T-cell (CD6)	Mouse anti-rat CD6	Serotec	1:30
B-cell (CD45R)	Mouse anti-rat CD45R	Serotec	1:30
Secondary antibodies			
PO399	Swine anti-rabbit IgG: HRP	Dako	1:100
M3007	Goat anti-mouse IgG: HRP	Caltag	1:100 + 1% rat serum
Star77	Goat anti-mouse IgG: HRP (rat absorbed)	Serotec	1:50
Star86P	Goat anti-mouse IgM: HRP	Serotec	1:100 + 1% rat serum
PO141	Rabbit anti–guinea pig IgG:HRP	Dako	1:50

HRP, horseradish peroxidase.

RESULTS

Large disorganized islets are present in 4-month-old diabetic GK pancreas. At the age of 4 months, total β-cell mass has been shown to be decreased by 60% in parallel to pancreatic insulin stores in GK rats as compared with Wistar rats (2). Two populations of islets were observed in GK rats: small islets with heavily stained β-cells and normal architecture (Fig. 1*A*) and large islets with spots of heterogeneously insulin-stained cells intermingled with fibrosis (Fig. 1*B*). This latter type of islet strongly differed from normal islets of age-matched Wistar control rats, where β-cells covered almost homogeneously the islet area, with only thin connective tissue spaces (Fig. 1*C*).

Gene expression analysis highlights the presence of an inflammatory/immune reaction in GK islets. We used Affymetrix microarrays to detect gene expression changes in islets of 4-month-old GK rats as compared with those of the nondiabetic Wistar controls. In GK islets, 71 genes were overexpressed and 19 genes were underexpressed as compared with Wistar control islets (Table 3). The analysis of the 71 overexpressed sequences according to known cellular function has led us to identify seven clusters: 23.9% of overexpressed genes are implicated in ECM/cell adhesion; 16.9% in inflammation; 16.9% in immune response; 2.8% in oxidative stress; 9.9% in metabolism; 5.6% in growth control, survival, and differentiation; and 23.9% are not classified (Table 3). ECM/cell adhesion, inflammation, immune response, and oxidative stress are the four principal families of potential interest in the context of our investigation. To validate our Affymetrix data, we selected a few genes: collagen I, collagen III, decorin, fibronectin, membrane-type 1 matrix metalloproteinase (also called MMP-14), and tissue inhibitor of metalloproteinase-1 for ECM/cell adhesion; annexin 1 (or lipocortin 1), lipocalin 2 (or neutrophil gelatinase-associated lipocalin), lipopolysaccharide-induced tumor necrosis factor α, and osteopontin for inflammation; CD53, CD74, and major histocompatibility complex (MHC) II for immune response; and thioredoxine-interacting protein and glutathione peroxidase for oxidative stress. The overexpression of all of these genes has been successfully confirmed by RT-PCR.

Fibrotic islet alterations result from mild and short-duration hyperglycemia. We selected antibodies against three proteins that belong to the ECM/cell adhesion family and had genes we found to be overexpressed in GK islets: collagen I and III and fibronectin. These antibodies were used for a immunohistochemical analysis of development of islet fibrosis as a function of duration of diabetes in GK rats.

At 1 month of age, islets of unweaned GK rats showed no sign of fibrosis as compared with control Wistar islets (14). However, at 2 months of age (i.e., after 1 month of chronic mild hyperglycemia), marked differences were observed (Fig. 1). In Wistar islets, fine labeling for collagen I and III and fibronectin, which are all known to be produced by vascular endothelial and/or smooth muscle cells (15,16) was present with intra- and peri-islet localization, therefore indicative of the presence of vessels (Fig. 1*D–F*). In GK islets, however, a peri- and intraislet thickening was observed in many medium-sized islets, and increased labeling of all the ECM components examined was observed: e.g., collagen I (Fig. 1*G* versus *D*, GK versus Wistar, respectively), collagen III (Fig. 1*H* versus *E*), and fibronectin (Fig. 1*I* versus *F*). In 4-month-old control Wistar rat islets, the labeling pattern for the various ECM molecules was similar to that described in 2-month-old Wistar rat islets (Fig. 1*J–L* versus *D–F* at 4 versus 2 months of age for collagen I and III and fibronectin, respectively). However, in 4-month-old GK rats, more precisely after 3 months of chronic hyperglycemia, when microarray analysis was performed, the largest islets showed massive fibrosis, as illustrated for collagen I (Fig. 1*M*), collagen III (Fig. 1*N*), and fibronectin (Fig. 1*O*). Nevertheless, some small and nonfibrotic islets were still present (Fig. 1*M*), which is in agreement with insulin labeling of GK islets (Fig. 1*A*).

Alteration of vascularization time correlates with hyperglycemia in GK islets. As described above, as early as 2 months of age (i.e., 1 month after diabetes onset),

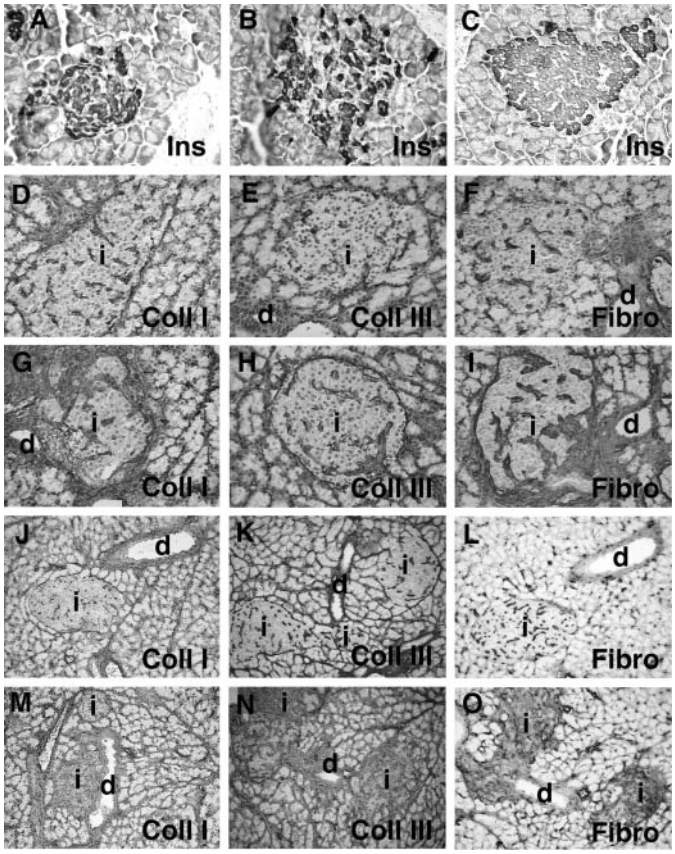

FIG. 1. Islet fibrosis progresses rapidly in mild hyperglycemic GK rats. Insulin labeling demonstrates the concomitant presence of small normal and large fibrotic islets (*A* and *B*, respectively) in 4-month-old GK pancreas as compared with age-matched control Wistar pancreas (*C*) (×500). As early as 1 month of chronic mild hyperglycemia (i.e., at 2 months of age), many GK islets show, compared with Wistar islets, peri- and intraislet thickening of vascularization, as demonstrated by labeling for collagen I (*G* versus *D*), collagen III (*H* versus *E*), or fibronectin (*I* versus *F*) (×500). At 4 months of age, fibrosis is extensive in large GK islets, as shown by collagen I (*M* versus *J* for GK and Wistar, respectively), collagen III (*N* versus *K*), and fibronectin (*O* versus *L*) labelings (×250). Of note, small intact islets coexist with large fibrotic islets, as shown in *M* (collagen I labeling), confirming the insulin data (*A* and *B*). d, duct; i, islet.

immunohistochemistry for the various ECM molecules suggested that vascularization might be the starting point of fibrosis formation in GK islets. Therefore, we compared the expression of a specific endothelial cell marker, von Willebrand factor (vWF), which is known to be increased in the blood of type 2 diabetic patients (10), on serial sections of 2-month-old Wistar and GK pancreata. Representative stainings for vWF and fibronectin of control Wistar islets are shown in Fig. 2*A* and *B*, respectively. As expected, Wistar islets are characterized by fine labeling of endothelial cells for both molecules. In age-matched GK pancreata, however, islet vascularization differed markedly from that of Wistar islets, as assessed by vWF labeling (Fig. 2*C*, *E*, and *G* versus *A*). Moreover, in a given GK rat pancreas, islets were extremely heterogenous in terms of vascularization; indeed, vessels appeared to be more or less hypertrophied (Fig. 2*C* and *E*) or even greatly disorganized (Fig. 2*G*). As demonstrated in Fig. 2*C* and *D*, for vWF and fibronectin, respectively, expression of both molecules is partially colocalized in midly hypertrophied vessels. Finally, while sized-matched GK islets showed different degrees of vascularization alteration (Fig.2*C*, *E*, and *G*), the extent of fibronectin labeling in corresponding serial sections greatly varied (Fig. 2*D*, *F*, and *H*).

Macrophage and granulocyte infiltration time correlates with hyperglycemia in GK islets. Our microarray data revealed that 16.9% of the genes that were found to be overexpressed in GK islets coded for molecules involved in immune response. Using quantitative RT-PCR, we confirmed the overexpression of three of these genes, namely CD53, CD74, and MHC class II (Table 3). Since MHC class II is a well-known macrophage marker (17), we investigated the presence of macrophages in the pancreata of both groups at the different ages. We used several antibodies that were available in rats: *1*) anti-MHC class II; *2*) ED1, which recognizes a 110-kD single-chain glycoprotein (human equivalent CD68), which is expressed predominantly on the lysosomal membrane of myeloid cells and is found on the majority of tissue macrophages and weakly on peripheral granulocytes (18); *3*) ED2, which reacts with a membrane antigen (human equivalent CD163) on resident rat macrophages (18); and *4*) ED3 (CD169), which recognizes a receptor for syalyated glycoconjugates and characterized tissue macrophage subpopulations involved in autoimmune disease (18). No difference was observed in 1-month-old Wistar and GK islets concerning MHC class II and CD68 islet labeling (data not shown). However, at 2 months of age (i.e., after 1 month of chronic mild hyperglycemia), labeling shows constantly more macrophages in/around GK islets than Wistar islets (Fig. 3*B* versus *A* for MHC class II, and Fig. 3*D* versus *C* for CD68). A similar observation has been done for both markers in 4-month-old animals of the two groups (14). However, at 4 months of age, macrophage GK islet infiltration appeared less pronounced than at 2 months. Using the ED2 macrophage antibody, no difference was observed between the two strains regardless of age, and macrophages recognized by the ED3 antibody were never detected (data not shown).

CD53 cell-surface antigen is a 43-kDa glycoprotein that is expressed by all myeloid and peripheral lymphoid B- and T-cells and also a small subset of thymocytes (19). In 1-month-old animals, $CD53^+$ cells were found to be located near the ducts, particularly in GK rats (data not shown). At 2 months of age, a more- or less-marked $CD53^+$ cell islet infiltration was observed in/around GK islets, while these cells were scarce in age-matched Wistar islets (Fig. 3*F* versus *E*). A similar observation has been done in 4-month-old GK pancreata, in which more $CD53^+$ cells were reproducibly found at the islet-ductal pole (data not shown). For a better characterization of this cell population, we used several antibodies against granulocytes (clone HIS48), mature T-cells (anti-CD6), or B-cells (anti-CD45R). At 2 months of age in both strains, T- and B- cells were exceptionally observed in (or close to) islets (data not shown). While granulocytes were scarce in 2-month-old Wistar pancreata (Fig. 3*G*), they were much more numerous in/around GK islets (Fig. 3*H*), thus confirming the myeloid phenotype of $CD53^+$ cells.

DISCUSSION

To investigate the mechanisms leading to fibrosis in GK islets, we performed a gene expression analysis using Affymetrix microarrays on islets of 4-month-old GK and age-matched control Wistar rats. Notably, around 60% of the genes that were overexpressed in 4-month-old GK rat islets (i.e., after 3 months of mild hyperglycemia) belong to ECM/cell adhesion (23.9%), inflammation (16.9%), immune

TABLE 3
List of genes modified in GK versus Wistar islets (Affymetrix analysis)

Gene overexpression

Gene ID number	Gene name	Gene symbol	Fold change	
			Affymetrix	RT-PCR
ECM/Cell adhesion				
AI169327	Tissue inhibitor of metalloproteinase 1	TIMP1	30.6	5.6
X70369	Collagen, type 3, α1	COL3A1	17.3	10
X05834	Fibronectin 1	FN1	10.3	11
AI231472	Collagen, type 1, α1	COL1A1	8.5	27
X62952	Vimentin	VIM	6.9	
X81449	Keratin 19	KRT19	6.4	
S77494	Lysyl oxidase	LOX	5.4	
AA892506	Coronin, actin-binding protein 1A	CORO1A	5.1	
X59859	Decorin	DCN	4.1	2.2
X89963	Thrombospondin 4	THBS4	4.0	
X83537	Matrix metalloproteinase 14, membrane inserted	MMP14	3.9	6.2
M83107	Transgelin	TAGLN	3.6	
AF016503	Procollagen C proteinase enhancer protein	PCOLCE	3.0	
AA892333	α Tubulin	TUBA6	2.8	
U75928	Secreted protein acidic and rich in cystein (osteonectin)	SPARC	2.5	
AF083269	Actin-related protein complex 1	ARPC1B	2.3	
X54617	Regulatory light-chain A gene for myosin regulatory light chain	RCL-A	2.2	
Inflammation				
AA946503	Lipocalin 2	LCN2	72.8	22
M98049	Pancreatitis-associated protein 1	PAP1	45.5	
M14656	Osteopontin	SPP1	14.9	17
L20869	Pancreatitis-associated protein 3	PAPIII0	9.0	
AI171962	Annexin 1 (p35) (lipocortin 1)	ANXA1	8.7	2
J02962	Lectin, galactose binding, soluble 3 (galectin 3)	LGALS3	6.2	
X17053	Immediate early serum responsive JE gene (macrophage chemoattractant protein-1)	JE	5.0	
D88250	Complement component 1, s subcomponent	C1S	3.2	
U53184	Lipopolysaccharide-induced tumor necrosis factor α	LITAF	2.4	2
AI136891	Zn finger protein 36, C3H type-like 1	ZFP3611	2.3	
L03201	Cathepsin S	CTSS	2.2	
X61381	Interferon inducible protein	IFITM3	2.2	
Immune response				
M12822	Ig germline κ-chain		17.4	
AA801174	Ig rearanged μ-chain C region		8.7	
AI234828	IgA heavy chain		4.3	
X13044	CD74 antigen	CD74	3.7	8
M57276	CD53 antigen	CD53	3.2	10
X68782	Ig heavy-chain VDJ region CH1-CH2		3.1	
U39609	Anti–nerve growth factor 30 antibody light chain		3.0	
AA850138	Ig active λ2-like chain		2.8	
M15562	Major histocompatibility complex class II RT1u D α chain		2.8	9
S81289	IgM κ-chain variable region		2.6	
X14254	Major histocompatibility complex class II associated invariant chain		2.5	
U75411	Anti-idiotype IgM light chain		2.5	
Oxidative stress				
AI237654	Upregulated by 1,25-dihydroxyvitamin D-3 (thioredoxin-interacting protein)	VDUP1	5.4	5.6
X07365	Gluthatione peroxidase 1	GPX1	2.7	2.2
Metabolism				
X15679	Preprotrypsinogen IV		17.9	
X02291	Aldolase B	ALDOB	11.9	
X59012	Trypsin V a-form		9.0	
D28560	Ectonucleotide pyrophosphatase/phosphodiesterase	ENPP2	3.7	
AA858673	Pancreatic secretory trypsin inhibitor type II	PSTI-II	3.6	
M54926	Lactate deshydrogenase A	LDHA	2.2	
D00753	Serine protease inhibitor	SPIN2C	2.0	

Continued on following page

TABLE 3
Continued

Gene overexpression

Gene ID number	Gene name	Gene symbol	Fold change	
			Affymetrix	RT-PCR
Not classified				
Growth control, survival, and differentiation				
E01983	Reg	REG	12.4	
D23676	Regenerating islet derived 3α	REG3A	11.1	
L13039	Calpactin I heavy chain	ANXA2	3.3	
U10071	Cocaine- and amphetamine-regulated transcript	CART	3.3	
D26307	Jun-D gene	JUND	13.1	
U32681	Deleted in malignant brain tumors 1	DMBT1	11.6	
AF014503	Nuclear protein 1	NUPR1	8.2	
AB012234	Nuclear factor I/X	NFIX	7.8	
AA875531	Cyclin-dependent kinase 110	CDK110	7.6	
D38380	Transferrin	TF	6.7	
J03627	S-100 related protein	S100a10	3.5	
M58716	Secretory granule membrane glycoprotein	GP2	3.2	
AI137583	Inhibitor DNA binding 2	ID2	3.1	
S87544	Polyprotein 1-microglobulin/bikunin	AMBP	2.9	
M27440	Apolipoprotein B	APOB	2.8	
AA899854	Topoisomerase (DNA) 2 α	TOP2A	2.7	
AA849769	Follistatin-related protein	FSTL1	2.7	
U95178	Disabled homolog 2, mitogen-responsive phophoprotein	DAB2	2.3	
X06916	S100 calcium binding protein A4	S100a4	2.3	
AF020757	Purinergic receptor P2X, ligand-gated ion channel, 2	P2RX2	2.3	
S76779	Apolipoprotein E	APOE	2.0	
ESTs 12 sequences				
8 Repetitive sequences				

Gene underexpression

Gene ID number	Gene name	Gene symbol	Fold change	
			Affymetrix	RT-PCR
AA848563	Heat shock protein 70-1	HSPA1A	16.7	
U48246	Protein kinase C binding protein NELL1	NELL1	16.1	
M72422	Glutamate decarboxylase 2	GAD2	4.9	
X70871	Cyclin G1	CCNG1	3.9	
M13588	Pancreatic polypeptide	PPY	3.7	
M15880	Neuropeptide Y	NPY	2.7	
J05592	Protein phosphatase 1, regulatory (inhibitor) subunit 1A	PPP1R1A	2.7	
U20796	Nuclear receptor subfamily 1, group D, member 2	NRLD2	2.6	
U08290	Neuronatin	NNAT	2.5	
M85214	Trk precursor	NTRK1	2.3	
E12625	sterol-C4-methyl oxidase like	SC4MOL	2.3	
M10094	RT1 class Ib gene	RT1AW2	2.3	
D85183	Protein tyrosine phosphatase	PTPNS1	2.2	
AA852004	Glutamine synthetase	GLUL	2.2	
L27075	ATP-citrate lyase	ACLY	2.2	
J03481	Quinoid dihydropteridine reductase	QDPR	2.1	
S75952	Glucagon-like peptide 1 receptor	GLP1R	2.1	
U17254	Immediate early gene transcription factor nerve growth factor-1B	NR4A1	2.1	
M23601	Monoamine oxidase B	MAOB	2.1	
ESTs 3 sequences				

response (16.9%), and oxidative stress (2.8%). For fifteen genes of interest, the relative expression levels were assessed by RT-PCR and found to be comparable to the microarray values.

While our gene analysis confirms the presence of fibrosis, more pertinently it highlights the presence of an inflammatory/immune reaction in islets of a nonobese animal model of spontaneous type 2 diabetes. But previously, no signs of inflammation had been described in the islets or acinar parenchyma of 3- to 3.5-month-old GK rats, while 28% of starfish islets were present (3). However, fibrosis is usually linked to inflammation and a common feature of type 2 diabetes in several animal models and also in humans (amyloid deposition) (4–8,20). Therefore, local islet inflammation might be a general phenomenom in type 2 diabetes, in addition to the presently well-

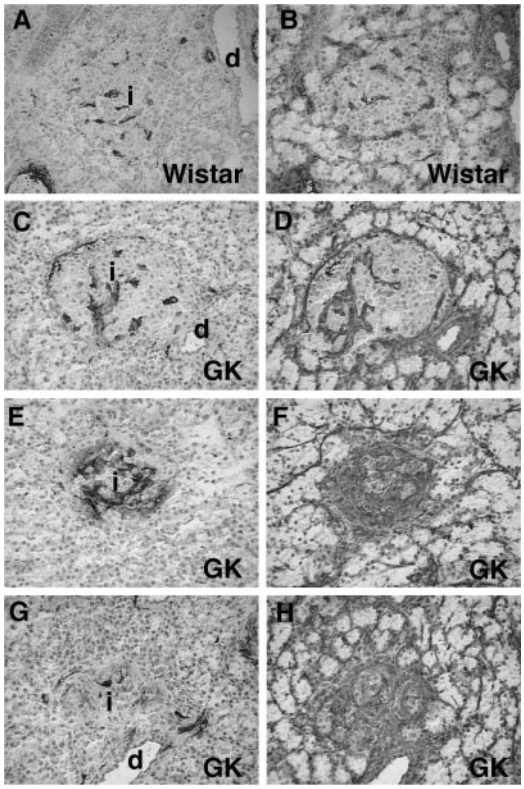

FIG. 2. Islet vascularization is altered in 2-month-old GK rats. Labelings for vWF (*left*) and fibronectin (*right*), two factors known to be produced by endothelial cells, show the normal organization of islet vascularization in 2-month-old Wistar rats (*A* and *B* for vWF and fibronectin, respectively). *C*, *E*, and *G*: Islet vascularization differs markedly in age-matched GK rats and appears to be either hypertrophied (*C* and *E*) or atrophied (G). At least in the first steps of the lesion formation, fibronectin and vWF labelings progress similarly (*C* versus *D*, for vWF and fibronectin, respectively), before invading the islet and desorganizing vascularization (*G* versus *H*) (×500).

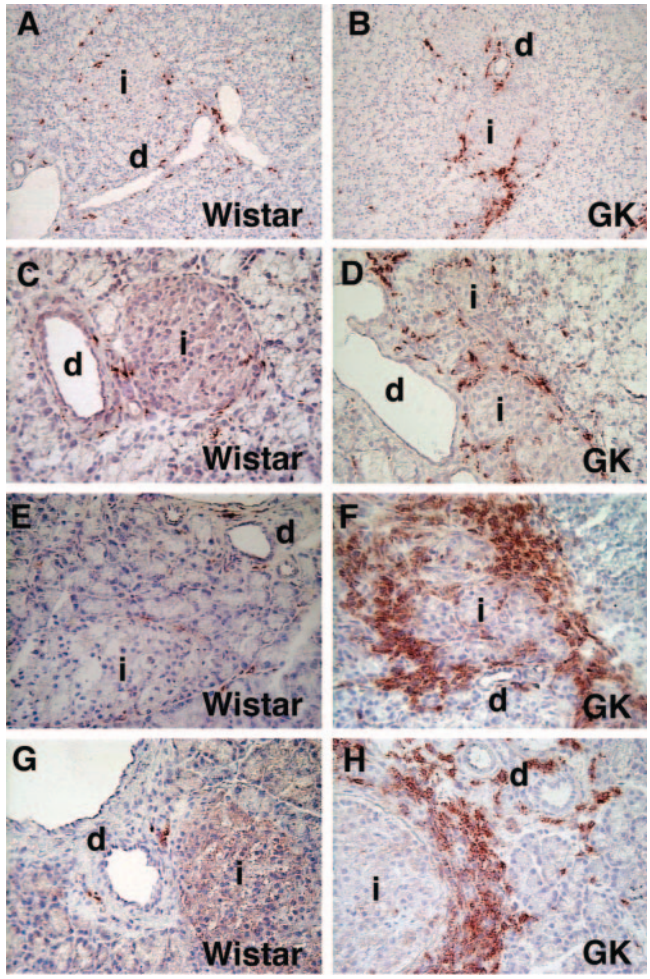

FIG. 3. Inflammatory cells rapidly infiltrate the islets of mildy hyperglycemic GK rats. Compared with 2-month-old Wistar rats, numerous macrophages are present in/around GK islets, as shown by MHC class II (*B* versus *A*; ×250) and CD68 labelings (*D* versus *C*; ×500). Other myeloid cells are also more abundant in GK islets, as demonstrated by CD53 (F versus *E*; ×500) and, particularly, granulocyte labeling (*H* versus *G*; ×500). The concomitant presence of macrophages and granulocytes together with the quasiabsence of T- and B-cells and ED3 macrophages that are involved in autoimmune reaction (data not shown) suggests a pure inflammatory process in this spontaneous model of type 2 diabetes, at least at this age.

acknowledged peripheral and adipose tissue inflammation (10).

However, at a given time, as shown here at 4 months of age (Fig. 1*M–O*), small (recently formed and not yet affected) and older, larger, more- or less-affected islets coexist. We also showed that islet fibrosis progresses with the duration of hyperglycemia. Since hyperglycemia is known to stimulate the secretion of fibronectin and collagen I and III by endothelial cells and/or vascular smooth muscle cells (15,16), we analyzed islet vascularization in Wistar and GK rats at various ages using vWF, a specific marker of endothelial cells (10). At 2 months of age, GK islet vascularization was heterogenous; it could be similar to that of Wistar islets, or more developed (in a way that is closely associated to fibronectin deposition) or greatly disorganized. These data suggest that ECM deposition progresses from intra- and peri-islet vessels, as it is known to happen in microangiopathy (21). Abnormalities of islet vascularization have been described in two other spontaneous models of type 2 diabetes, namely OLETF and SDT rats, but these alterations were not detected in a colony of GK rats that differ from ours (5,6,22). In humans, amyloid deposition exists as "perivascular deposits adjacent to capillaries surrounding the islet or those penetrating the islet core with limited accumulation or extensive deposits within the islet" (8).

Altered vascularization and abnormal blood flow have been described in spontaneous animal models of type 2 diabetes, particularly GK and OLETF rats (11,23–26). Increased islet blood flow, which is present in young diabetic GK rats, is reverted to decreased flow when animals reach the age of 1 year (23). In OLETF rats, increased islet blood flow is also observed during the pre-diabetic phase (26), and, as the rats advance in age, the fine capillaries that form the intraislet network are extremely sparse in the lean diabetic group as compared with the age-matched obese OLETF group or control Long-Evans Tokushima Otsuka (LETO) group (25). In GK rats, early increased capillary blood flow might be one of the factors that will damage the islet endothelium, induce thickening of the capillary walls, reduce islet blood flow, as described in diabetic retina and kidneys, and finally contribute to decline of islet function (24). Therefore, we looked for genes that are overexpressed in GK islets and belong to the families depicted above but are also expressed normally in endothelial and vascular smooth muscle cells and involved in angiogenesis and atherosclerosis. Decorin, galectin 3 (or lectin galactose binding, soluble 3) (Table 3), tissue inhibitor of metalloprotein-

ase-1, and membrane-type 1 matrix metalloproteinase are known to be involved in angiogenesis and/or atherosclerosis (27–30). In addition expression of osteopontin or galectin 3 is increased in human diabetic arteries and/or under high glucose concentration in rat aortic diabetic arteries and/or also under high glucose concentration in rat aortic smooth muscle (27,31,32).

Endothelial dysfunction is the hallmark of diabetes complications regardless of its type (33,34). Indeed, hyperglycemia is known to activate intra- and peri-islet endothelial cells, leading to proinflammatory cytokine production and adhesion molecule expression that facilitate the recruitment, adhesion, and migration of leukocytes (35–38). In GK kidney and aorta, endothelial modifications have been described where they are associated with monocyte/macrophage infiltration and increased macrophage-induced angiogenesis, respectively (39,40). Our immunohistochemical data reveal the presence of more MHC class II^+ and $CD68^+$ macrophages in and/or around GK islets than in those of Wistar at 2 and 4 months of age. More $CD68^+$ macrophages are also present in human type 2 diabetes islets (J. Ehses, A. Perren, M. Donath, personal communication). In addition, we found overexpression of the gene for CD74 (macrophage inhibitory factor receptor): CD74 coexists with CD68 on macrophages (41,42). Finally, $ED3^+$ macrophages and mature T- and B-cells are absent in the early phase of the disease, arguing against a precocious autoimmune reaction in this type 2 diabetic model.

Activated macrophages produce various ECM-related molecules, chemokines (and their receptors), inflammatory cytokines, and growth factors (43,44). The secretion of some inflammatory factors such as interleukin-1 and -6, tumor necrosis factor α, transforming growth factor β1, and macrophage chemoattractant protein by monocytes/macrophages is stimulated by hyperglycemia (45,46). From our gene expression analysis (Table 3), overexpression of some other genes might be attributed to effect on, or production by, islet macrophages: this is the case for immediate early serum-responsive JE gene that corresponded to macrophage chemoattractant protein-1 gene and genes coding for proinflammatory factors, such as lipopolysaccharide-induced tumor necrosis factor α (47) and galectin 3 (48), or anti-inflammatory factors, such as apolipoprotein E (49) and lipocortin 1 (annexin 1) (50) and also transferrin, a circulating negative acute-phase protein that is downregulated in inflammatory conditions such as diabetes (51) and might be of macrophage origin (43).

An impressive infiltration of cells positive for CD53 (another gene that was found to be overexpressed in GK islets) is present in diabetic GK pancreata. These $CD53^+$ cells correspond to granulocytes and not to peripheral lymphocytes. Notably, macrophage (and endothelium)-produced galectin 3 is known to facilitate binding of neutrophils to the endothelium (48). Activated granulocytes are potential producers of toxic oxygen metabolites, lytic and toxic proteases, nitric oxide, and inflammatory cytokines (52). These data are also in line with the gene overexpression for lipocaline 2 (neutrophil gelatinase–associated lipocalin) (Table 3), which is produced mainly by granulocytes. Lipocalin 2 is considered a sign of leukocyte activation in various diseases, particularly hypertension and acute cerebral ischemic attack (53). In addition, lipocortin 1 (or annexin 1), as mentioned above for macrophages, is also produced by granulocytes (54). Finally, granulocytes are associated with capillary closure in spontaneously diabetic monkey retinas (55), and granulocytes might play a role in atherosclerosis (56).

In conclusion, our data demonstrate, for the first time, that an inflammatory reaction takes place at the islet level in a type 2 diabetic animal model, resembling microangiopathy with subsequent fibrosis leading to loss of islet architecture and probably responsible for increased β-cell impairment. In various type 2 diabetic animal models, treatments that preserve islet architecture, thiazolinediones (rosiglitazone), ACE inhibitor (ramipril), and protease inhibitor (camostat) improve β-cell function (5,20,57,58). Also, glitazones ameliorate endothelial dysfunction in patients with diabetes and lower inflammatory markers and reactive oxygen species in serum (59). Therefore, our data contributing to a better understanding of the pathogenesis of the disease might lead to design β-cell–sensitizing molecules with improved anti-inflammatory and anti-atherosclerotic effects.

ACKNOWLEDGMENTS

This work was supported in parts by grants from the National Center for Scientific Research and the Swiss National Science Foundation. S.C. was a recipient of doctoral fellowships from the Ministère de l'Education Nationale, de l'Enseignement et de la Recherche, and from the Fondation pour la recherche médicale. S.C. also thanks Naturalia et Biologia Association for a travel grant.

Parts of this work were presented at the 18th International Diabetes Federation Congress, Paris, France, 24–29 August 2003 and at the 41st Annual Meeting of the European Association of the Study of Diabetes, Athens, Greece, 12–15 September 2005.

REFERENCES

1. Kakizaki M, Fujiya H, Goto Y: The pancreatic islets of the spontaneous diabetic rats. *Diabetes* 7:23–25, 1979
2. Movassat J, Saulnier C, Serradas P, Portha B: Impaired development of pancreatic beta-cell mass is a primary event during the progression to diabetes in the GK rat. *Diabetologia* 40:916–925, 1997
3. Hoog A, Hu W, Abdel-Halim SM, Falkmer S, Qing L, Grimelius L: Ultrastructural localization of insulin-like growth factor-2 (IGF-2) to the secretory granules of insulin cells: a study in normal and diabetic (GK) rats. *Ultrastruct Pathol* 21:457–466, 1997
4. Pick A, Clark J, Kubstrup C, Levisetti M, Pugh W, Bonner-Weir S, Polonsky KS: Role of apoptosis in failure of beta-cell mass compensation for insulin resistance and β-cell defects in the male Zucker diabetic fatty rat. *Diabetes* 47:358–364, 1998
5. Ko SH, Kwon HS, Kim SR, Moon SD, Ahn YB, Song KH, Son HS, Cha BY, Lee KW, Son HY, Kang SK, Park CG, Lee IK, Yoon KH: Ramipril treatment suppresses islet fibrosis in Otsuka Long-Evans Tokushima fatty rats. *Biochem Biophys Res Commun* 316:114–122, 2004
6. Masuyama T, Komeda K, Hara A, Noda M, Shinohara M, Oikawa T, Kanazawa Y, Taniguchi K: Chronological characterization of diabetes development in male Spontaneously Diabetic Torii rats. *Biochem Biophys Res Commun* 314:870–877, 2004
7. Like AA, Chick WL: Studies in the diabetic mutant mouse: II. Electron microscopy of pancreatic islets. *Diabetologia* 6:216–242, 1970
8. Clark A, Nilsson MR: Islet amyloid: a complication of islet dysfunction or an aetiological factor in type 2 diabetes? *Diabetologia* 47:157–169, 2004
9. Donath MY, Storling J, Maedler K, Mandrup-Poulsen T: Inflammatory mediators and islet beta-cell failure: a link between type 1 and type 2 diabetes. *J Mol Med* 81:455–470, 2003
10. Kolb H, Mandrup-Poulsen T: An immune origin of type 2 diabetes? *Diabetologia* 48:1038–1050, 2005
11. Atef N, Portha B, Penicaud L: Changes in islet blood flow in rats with NIDDM. *Diabetologia* 37:677–680, 1994
12. Portha B, Giroix MH, Serradas P, Gangnerau MN, Movassat J, Rajas F, Bailbe D, Plachot C, Mithieux G, Marie JC: β-Cell function and viability in the spontaneously diabetic GK rat: information from the GK/Par colony. *Diabetes* 50 (Suppl. 1):S89–S93, 2001

13. Lilla V, Webb G, Rickenbach K, Maturana A, Steiner DF, Halban PA, Irminger JC: Differential gene expression in well-regulated and dysregulated pancreatic beta-cell (MIN6) sublines. *Endocrinology* 144:1368–1379, 2003
14. Homo-Delarche F, Calderari S, Irminger J, Coulaud J, Rickenbach K, Gangnerau M, Portha B, Serradas P: Chronic hyperglycemia is associated with an inflammatory islet reaction in a spontaneous model of type 2 diabetes (T2D) (Abstract). *Diabetologia* 48 (Suppl. 1):A180, 2005
15. Raines EW: The extracellular matrix can regulate vascular cell migration, proliferation, and survival: relationships to vascular disease. *Int J Exp Pathol* 81:173–182, 2000
16. Xin X, Khan ZA, Chen S, Chakrabarti S: Extracellular signal-regulated kinase (ERK) in glucose-induced and endothelin-mediated fibronectin synthesis. *Lab Invest* 84:1451–1459, 2004
17. Grabowska A, Lampson LA: MHC expression in nonlymphoid tissues of the developing embryo: strongest class I or class II expression in separate populations of potential antigen-presenting cells in the skin, lung, gut, and inter-organ connective tissue. *Dev Comp Immunol* 19:425–450, 1995
18. Voorbij HA, Jeucken PH, Kabel PJ, De Haan M, Drexhage HA: Dendritic cells and scavenger macrophages in pancreatic islets of prediabetic BB rats. *Diabetes* 38:1623–1629, 1989
19. Tomlinson MG, Williams AF, Wright MD: Epitope mapping of anti-rat CD53 monoclonal antibodies. Implications for the membrane orientation of the transmembrane 4 superfamily. *Eur J Immunol* 23:136–140, 1993
20. Finegood DT, McArthur MD, Kojwang D, Thomas MJ, Topp BG, Leonard T, Buckingham RE: β-Cell mass dynamics in Zucker diabetic fatty rats: rosiglitazone prevents the rise in net cell death. *Diabetes* 50:1021–1029, 2001
21. Schalkwijk CG, Stehouwer CD: Vascular complications in diabetes mellitus: the role of endothelial dysfunction. *Clin Sci (Lond)* 109:143–159, 2005
22. Kampf C, Bodin B, Kallskog O, Carlsson C, Jansson L: Marked increase in white adipose tissue blood perfusion in the type 2 diabetic GK rat. *Diabetes* 54:2620–2627, 2005
23. Svensson AM, Ostenson CG, Jansson L: Age-induced changes in pancreatic islet blood flow: evidence for an impaired regulation in diabetic GK rats. *Am J Physiol Endocrinol Metab* 279:E1139–E1144, 2000
24. Carlsson PO, Jansson L, Ostenson CG, Kallskog O: Islet capillary blood pressure increase mediated by hyperglycemia in NIDDM GK rats. *Diabetes* 46:947–952, 1997
25. Mizuno A, Noma Y, Kuwajima M, Murakami T, Zhu M, Shima K: Changes in islet capillary angioarchitecture coincide with impaired B-cell function but not with insulin resistance in male Otsuka-Long-Evans-Tokushima fatty rats: dimorphism of the diabetic phenotype at an advanced age. *Metabolism* 48:477–483, 1999
26. Iwase M, Uchizono Y, Tashiro K, Goto D, Iida M: Islet hyperperfusion during prediabetic phase in OLETF rats, a model of type 2 diabetes. *Diabetes* 51:2530–2535, 2002
27. Seki N, Hashimoto N, Sano H, Horiuchi S, Yagui K, Makino H, Saito Y: Mechanisms involved in the stimulatory effect of advanced glycation end products on growth of rat aortic smooth muscle cells. *Metabolism* 52:1558–1563, 2003
28. Schonherr E, Sunderkotter C, Schaefer L, Thanos S, Grassel S, Oldberg A, Iozzo RV, Young MF, Kresse H: Decorin deficiency leads to impaired angiogenesis in injured mouse cornea. *J Vasc Res* 41:499–508, 2004
29. Strom A, Ahlqvist E, Franzen A, Heinegard D, Hultgardh-Nilsson A: Extracellular matrix components in atherosclerotic arteries of Apo E/LDL receptor deficient mice: an immunohistochemical study. *Histol Histopathol* 19:337–347, 2004
30. Haas TL: Endothelial cell regulation of matrix metalloproteinases. *Can J Physiol Pharmacol* 83:1–7, 2005
31. Takemoto M, Yokote K, Nishimura M, Shigematsu T, Hasegawa T, Kon S, Uede T, Matsumoto T, Saito Y, Mori S: Enhanced expression of osteopontin in human diabetic artery and analysis of its functional role in accelerated atherogenesis. *Arterioscler Thromb Vasc Biol* 20:624–628, 2000
32. Akahane T, Akahane M, Shah A, Thorgeirsson UP: TIMP-1 stimulates proliferation of human aortic smooth muscle cells and Ras effector pathways. *Biochem Biophys Res Commun* 324:440–445, 2004
33. Calles-Escandon J, Cipolla M: Diabetes and endothelial dysfunction: a clinical perspective. *Endocr Rev* 22:36–52, 2001
34. Brownlee M: Biochemistry and molecular cell biology of diabetic complications. *Nature* 414:813–820, 2001
35. Morigi M, Angioletti S, Imberti B, Donadelli R, Micheletti G, Figliuzzi M, Remuzzi A, Zoja C, Remuzzi G: Leukocyte-endothelial interaction is augmented by high glucose concentrations and hyperglycemia in a NF-kB-dependent fashion. *J Clin Invest* 101:1905–1915, 1998
36. Booth G, Stalker TJ, Lefer AM, Scalia R: Elevated ambient glucose induces acute inflammatory events in the microvasculature: effects of insulin. *Am J Physiol Endocrinol Metab* 280:E848–E856, 2001
37. Biedermann BC: Vascular endothelium: checkpoint for inflammation and immunity. *News Physiol Sci* 16:84–88, 2001
38. Takaishi H, Taniguchi T, Takahashi A, Ishikawa Y, Yokoyama M: High glucose accelerates MCP-1 production via p38 MAPK in vascular endothelial cells. *Biochem Biophys Res Commun* 305:122–128, 2003
39. Kobayashi S, Kimura I, Kimura M: Diabetic state-modified macrophages in GK rat release platelet-derived growth factor-BB for tube formation of endothelial cells in rat aorta. *Immunopharmacology* 35:171–180, 1996
40. Bitar MS, Wahid S, Mustafa S, Al-Saleh E, Dhaunsi GS, Al-Mulla F: Nitric oxide dynamics and endothelial dysfunction in type II model of genetic diabetes. *Eur J Pharmacol* 511:53–64, 2005
41. Nagashima R, Maeda K, Imai Y, Takahashi T: Lamina propria macrophages in the human gastrointestinal mucosa: their distribution, immunohistological phenotype, and function. *J Histochem Cytochem* 44:721–731, 1996
42. Leng L, Metz CN, Fang Y, Xu J, Donnelly S, Baugh J, Delohery T, Chen Y, Mitchell RA, Bucala R: MIF signal transduction initiated by binding to CD74. *J Exp Med* 197:1467–1476, 2003
43. Nathan CF: Secretory products of macrophages. *J Clin Invest* 79:319–326, 1987
44. Homo-Delarche F, Drexhage HA: Immune cells, pancreas development, regeneration and type 1 diabetes. *Trends Immunol* 25:222–229, 2004
45. Shanmugam N, Reddy MA, Guha M, Natarajan R: High glucose-induced expression of proinflammatory cytokine and chemokine genes in monocytic cells. *Diabetes* 52:1256–1264, 2003
46. Devaraj S, Venugopal SK, Singh U, Jialal I: Hyperglycemia induces monocytic release of interleukin-6 via induction of protein kinase c-α and -β. *Diabetes* 54:85–91, 2005
47. Bolcato-Bellemin A, Mattei M, Fenton M, Amar S: Molecular cloning and characterization of mouse LITAF cDNA: role in the regulation of tumor necrosis factor-alpha (TNF-alpha) gene expression. *J Endotoxin Res* 10:15–23, 2004
48. Almkvist J, Karlsson A: Galectins as inflammatory mediators. *Glycoconj J* 19:575–581, 2004
49. Larkin L, Khachigian LM, Jessup W: Regulation of apolipoprotein E production in macrophages (Review). *Int J Mol Med* 6:253–258, 2000
50. Perretti M: Endogenous mediators that inhibit the leukocyte-endothelium interaction. *Trends Pharmacol Sci* 18:418–425, 1997
51. Gomme PT, McCann KB, Bertolini J: Transferrin: structure, function and potential therapeutic actions. *Drug Discov Today* 10:267–273, 2005
52. Xiao H, Heeringa P, Liu Z, Huugen D, Hu P, Maeda N, Falk RJ, Jennette JC: The role of neutrophils in the induction of glomerulonephritis by anti-myeloperoxidase antibodies. *Am J Pathol* 167:39–45, 2005
53. Xu S, Venge P: Lipocalins as biochemical markers of disease. *Biochim Biophys Acta* 1482:298–307, 2000
54. Perretti M, Flower RJ: Annexin 1 and the biology of the neutrophil. *J Leukoc Biol* 76:25–29, 2004
55. Kim SY, Johnson MA, McLeod DS, Alexander T, Hansen BC, Lutty GA: Neutrophils are associated with capillary closure in spontaneously diabetic monkey retinas. *Diabetes* 54:1534–1542, 2005
56. Langheinrich AC, Bohle RM: Atherosclerosis: humoral and cellular factors of inflammation. *Virchows Arch* 446:101–111, 2005
57. Diani AR, Sawada G, Wyse B, Murray FT, Khan M: Pioglitazone preserves pancreatic islet structure and insulin secretory function in three murine models of type 2 diabetes. *Am J Physiol Endocrinol Metab* 286:E116–E122, 2004
58. Jia D, Taguchi M, Otsuki M: Synthetic protease inhibitor camostat prevents and reverses dyslipidemia, insulin secretory defects, and histological abnormalities of the pancreas in genetically obese and diabetic rats. *Metabolism* 54:619–627, 2005
59. Sjoholm A, Nystrom T: Endothelial inflammation in insulin resistance. *Lancet* 365:610–612, 2005